Powder Technology 390 (2021) 330–338

Contents lists available at ScienceDirect

Powder Technology

journal homepage: www.elsevier.com/locate/powtec

Rapid vacuum-driven monolayer assembly of microparticles on the surface of perforated microfluidic devices

Nathaniel Berneman [a,b,1], Ignaas Jimidar [a,b,1], Ward Van Geite [a], Han Gardeniers [b], Gert Desmet [a,*]

[a] Department of Chemical Engineering CHIS, Vrije Universiteit Brussel, Brussels 1050, Belgium
[b] Mesoscale Chemical Systems, University of Twente, Enschede 7522 NB, the Netherlands

ARTICLE INFO

Article history:
Received 27 January 2021
Received in revised form 20 May 2021
Accepted 21 May 2021
Available online 28 May 2021

Keywords:
Directed assembly
Microparticles
Ordered arrays
Open microfluidics

ABSTRACT

On the cusp of a miniaturized device era, a number of promising methods have been developed to attain large-scale assemblies of micro- and nanoparticles. In this study, a novel method is proposed to firmly capture dispersed microparticles of nominal sizes of 10 μm on a two-dimensional array (1.0×1.0 mm^2) of through-pores on a surface. This is obtained by dispensing a droplet of the particle dispersion on the pores, which drains by applying a vacuum-driven force at the backside of the pores. The assembled particles are captured on the surface in a reversible way, making them available for direct manipulation and inspection, or subsequent transfer of the particles to a second surface. The relevant process parameters dispersant concentration, dispersant type, particle properties, and pitch distance d, are optimized to obtain (near-)perfect ordered particle arrays. Furthermore, to significantly improve the quality of the particle assembly, washing steps are added to remove excess particles from the surface. Silica or polystyrene (PS) particle assemblies with an error ratio (ER) as low as 0.2% are obtained, demonstrating the universality of the proposed method. For the smallest pitch, $d = 1.25$ μm, even with optimal process parameters, higher ER-values (=1.1%) are obtained.

© 2021 Elsevier B.V. All rights reserved.

1. Introduction

The construction of functional structures and devices accomplished by positioning spherical microparticles in large ordered two-dimensional (2D) arrangements has attracted much interest in the scientific community [1] and has demonstrated its potential as a platform for the development of applications in numerous fields, ranging from colloidal lithography to biomolecular assays [2–17].

A multitude of existing techniques uses physical boundaries, in the form of wells, walls or confined microfluidic chips, as a strategy to trap particles or cells onto a designed grid [7,18–20]. However, these techniques limit the accessibility of trapped particles or their potential manipulation or transferability. Some methods depend on particle specific-properties, for instance, applying an electromagnetic field for directed assembly of microparticles is restricted to the use of polarizable particles [21–25].

Additionally, the ability to firmly secure the particles or cells in their ordered positions when exerting external forces (e.g., a liquid flow), and to release them if needed (e.g., for transfer) in a controlled manner, is a prerequisite for broad applicability and versatility. Koh et al. [26] have shown the benefit of transferability of particles as they developed a dry rubbing method to produce large areas of ordered particles onto rigid patterned substrates, which can then be transferred on a flexible rubber substrate. These large-area flexible substrates have been utilized as photomasks to produce various photoresist patterns. Py et al. [27] have developed a grid of patch-clamp traps integrated inside a microfluidic chip, to trap neuronal cells onto specific positions recreating neural networks. This technique enabled them to study the effect of applied physicochemical stimuli, such as a flow of dissolved drugs, on cells. However, if the patch-clamp system did not vigorously hold the cells in-place, the dynamic flow would displace the cells and disturb the cellular network.

In the present work, we propose a novel rapid, universal and scalable method to assemble spherical microparticles on 2D micromachined arrays of membrane pores. By applying a vacuum-driven force across a suction membrane perforated with an ordered array of through-pores, microparticles dispersed in a solvent can be rapidly assembled and reversibly captured in ordered arrangements on a (flat) surface. As the vacuum force can be controlled at all time, the assembled microparticle array is readily available for subsequent manipulation, release and transfer. The assembly technique has been demonstrated using different particle types and dispersants, making it suitable for a wide variety of microparticle applications e.g., microlens arrays, flexible electronic devices, or potentially also cell-based applications.

* Corresponding author.
E-mail addresses: i.s.m.jimidar@utwente.nl (I. Jimidar), gedesmet@vub.be (G. Desmet)

[1] These authors contributed equally.

https://doi.org/10.1016/j.powtec.2021.05.079
0032-5910/© 2021 Elsevier B.V. All rights reserved.

2. Experimental section

2.1. Materials

Experiments were performed with monodisperse hydrophilic silica (1.85 g cm^{-3}) particles with diameter (9.98 ± 0.31 μm) and hydrophobic polystyrene particles (1.05 g cm^{-3}) with diameter (9.98 ± 0.11 μm), both purchased in a 50 mg mL^{-1} aqueous dispersion from microParticles GmbH (Germany). The mentioned standard deviation (SD) in particle size was specified by the supplier and taken for granted. The suction membranes were fabricated using a sequence of different techniques used in developing MEMS devices (cf. fabrication details for perforated membranes in SI). The pores of the micromachined membrane were distributed over an area of 1.0 × 1.0 mm^2 on the silicon chip with a size of 14 × 14 mm^2. The diameter of the membrane pore is 7.5 ± 0.2 μm. The SD in the pore sizes originates from the non-uniformity of the wafer-scale etching process. The particle-to-particle distance, pitch *d*, was varied. The micromachined pores are arranged on a hexagonal array. To change the chemical nature of the surface of the silicon membranes, they were coated with a hydrophobic CF_X-layer (2≤x≤3) [28]. The CF_X-coating was deposited on the membranes by plasma polymerization of CHF_3 confined in a reactive ion etcher (RIE) system (25 sccm CHF_3, 11 W, 130 mTorr, 8 min., electrode temp. 20 °C) [29].

2.2. Setup and operating principle

In order to apply the vacuum-driven suction-force through the membrane pores, a tailored setup was built Fig. S4 in SI). Optomechanical parts were purchased from Thorlabs GmbH (Germany) to create the supporting structure of the setup, while a vacuum chuck was designed in-house and outsourced for production through 3D Hubs BV (The Netherlands). The vacuum chuck includes a dual-channel design, providing one channel to hold the chip in place using vacuum, and a separate channel allowing the control of the suction-force passing through the particle trapping pores. A set of two synthetic rubber Viton® o-rings, with internal diameters 6.0 and 12.0 mm respectively and thickness of 1.0 mm, were purchased from ERIKS NV (Belgium), to assure a leakproof vacuum seal between the chip and vacuum chuck.

3. Results and discussion

Fig. 1 schematically represents the proposed method, using a suction membrane chip that can be either placed in a horizontal (Fig. 1a) or vertical direction (Fig. 1b). In both cases, a specified volume (ranging from 25.0 μL to 1.8 mL) of the particle dispersion is manually dispensed on the chip using a micropipette. In the present study, the diameter of the droplets varied between 4 and 18 mm, corresponding to a width that is at least 3 up to 11 times larger than the suction membrane's diagonal.

In the horizontal mode, the droplets were deposited directly on top of a 1.0 × 1.0 mm^2 membrane (cf. Fig. 1a1). In the vertical mode, the droplets were dispensed close to the top edge of the membrane, leading to the formation of a narrow stream of liquid flowing across the membrane (cf. Fig. 1b1). The width of the stream is approximately 1.1 mm, determined by the diameter of the pipette tip opening. In the horizontal mode, the vacuum channel connected to the pores was opened immediately after the deposition of a droplet (cf. Fig. 1a1), whereas in the vertical position the vacuum was applied while the droplet was being dispensed (cf. Fig. 1b1). As illustrated in Fig. 1a2 & 1b2, particles assemble on the pore orifices while the droplet is vanishing through the pores, with a few excess particles remaining on the chip. Note that the pore size is significantly smaller than the diameter of the smallest monodisperse particles used in the experiments, preventing clogging of the

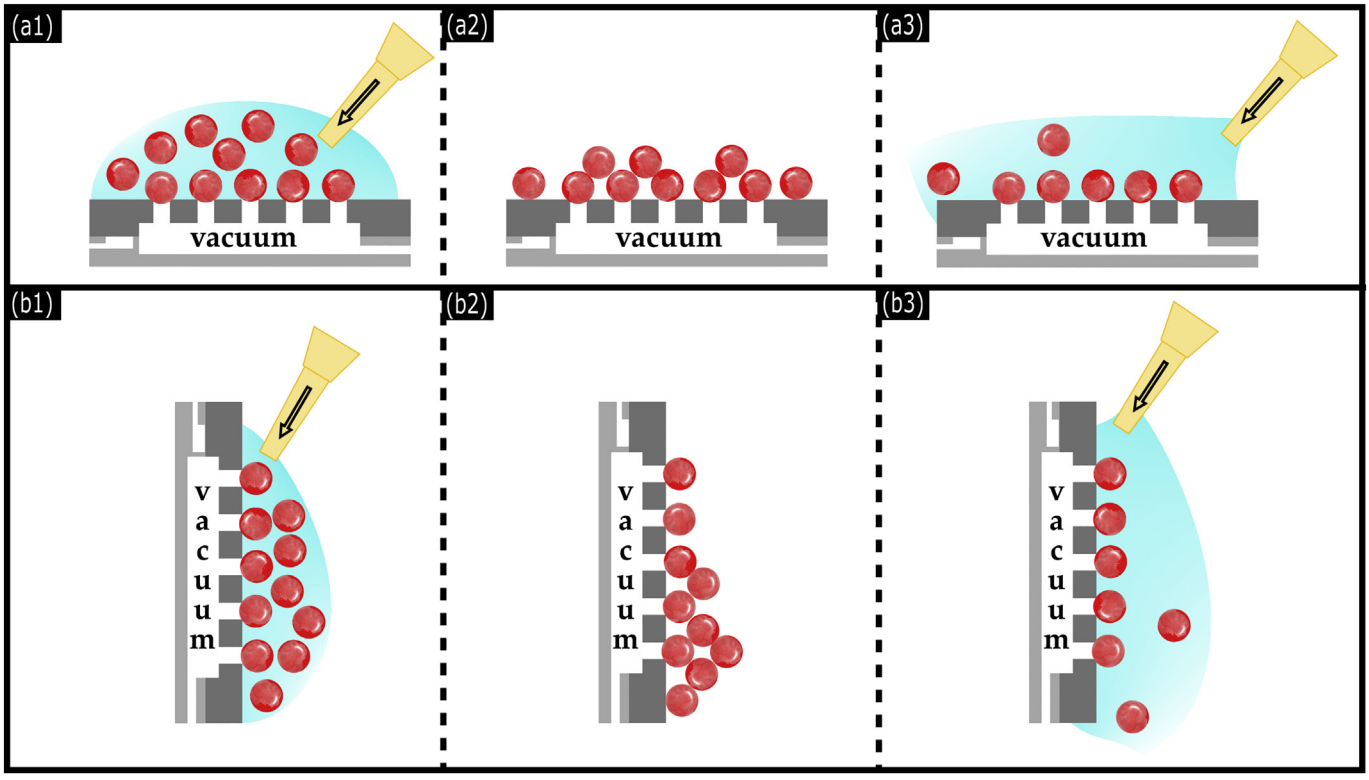

Fig. 1. Schematic representation of the experimental setup placed in **(a)** horizontal position and **(b)** vertical position. The perforated silicon chip with pores (dark grey) is fixed on an aluminum chuck (light grey) through which a vacuum force is applied, draining the dispersant from the surface of the chip. **(1)** A droplet of a particle dispersion with volume *V* and concentration *c* is dispensed on the silicon chip (dark grey) using a micropipette. Due to the applied vacuum force, the droplet is sucked through the pores with particles assembling on the pores **(2)**. Potentially formed clusters in **(2)** are removed by dispensing a sufficiently large droplet **(3)** of liquid dragging any excess particles off the chip.

pores. The typical timescale for the droplets to be completely or partially sucked into the pores was 5–8 s, depending on the volume of the droplet.

The total number of particles occupying the membrane depends on the total relative loading (TRL) of particles dispensed on the chip. The latter is determined by the the number of dispensed droplets N, and the concentration c of the dispersion. The TRL is then defined as TRL $= N\times$ RL_1, where RL_1 denotes the relative loading of a single droplet (cf. Eq. (1)).

To relate the number of particles present in a single dispensed droplet ($N = 1$) to the number of membrane pores, a relative loading RL_1 is defined:

$$RL_1 = \frac{\text{number of particles in the dispersion droplet}}{\text{number of membrane pores on the chip}} \quad (1)$$

As the particles are held firmly in place, a flow of water or ethanol (1 mL) can be applied across the chip's surface to wash away excess particles or dust contaminants, while still applying the vacuum-force to the pores (Fig. 1a3 & 1b3). If needed, the loading and washing step can be repeated to assemble particles on the remaining open pores of the membrane.

To aim for a given RL_1, the volume V of the dispensed droplets was adapted according to the concentration of the particle dispersion c. The dispersion is continuously stirred to obtain a homogeneous distribution of particles. Droplets are drawn from this stirred dispersion using a micropipette, allowing the control of the RL_1 value of the dispensed droplet.

3.1. General observations and effect of total relative load, particle concentration and number of application steps

The first set of experiments was performed by dispensing single water droplets containing silica particles ($c = 0.005$ mg mL^{-1}, $RL_1 \cong 1.0$) on chips with a through-pore pattern with a pitch $d = 35$ μm (diameter through-pores $= 7.5 \pm 0.2$ μm). As can be observed in Fig. 2 this leads to the formation of an ordered array of silica particles. The formed particle assembly is however not perfect, neither in the horizontal nor the vertical mode. Figs. 2 and S3 (cf. SI) show the occurrence of three distinct types of defects: particle clusters of various sizes (blue-colored circles), empty pores (red-colored circles), and dust contamination (green-colored circles). Some orifices inevitably draw more than one particle, due to the random distribution of the particles in the liquid. This explains the formation of the clusters. Similarly, the uneven distribution of the particles also leads to several pores remaining open after the entire droplet has vanished.

To quantify the occurrence of these defects, the error ratio ER was defined as:

$$ER = \frac{\text{number of empty pores} + \text{number of clusters}}{\text{total number of membrane pores-dust blocked pores}} \quad (2)$$

In this definition, pores blocked by occasional dust particles are excluded, as we consider the interference of dust particles as random, unpredictable contaminations which would be absent when working under 100% dust-free conditions. As a matter of reference, the ER-values of the particle assembly displayed in Fig. 2 correspond to ER = 3.8% vs. incl. dust $ER_{dust} = 4.1\%$ (Fig. 2a) and ER=1.9% vs. incl. dust $ER_{dust} = 2.7\%$ (Fig. 2b).

To investigate to what extent the particle concentration c affects the error ratio ER, experiments were performed with single water droplets carrying different silica particle concentrations, keeping the same $RL_1 \cong 1.0$. The results presented in Fig. S4 (cf. SI) highlight that depending on the operating mode, the relative loading in conjunction with the dispersion concentration c affect the error ratio, i.e., the quality of the assembled array of particles. To keep the RL_1 constant, lower volume droplets are dispensed at higher concentrations. Consequently, the local concentration of particles in the vicinity of the membrane pores is higher, i.e., the effective RL. Therefore, at higher concentrations the formation of clusters is promoted, while in the most diluted case the number of empty pores is more pronounced.

Altogether, these results (cf. Figs. 2 & S4) show that two major issues should be addressed in order to improve the quality of the assembled particle arrays: avoiding the presence of clusters and decreasing the number of empty pores. Intuitively, the formation and presence of clusters can be minimized by avoiding high concentrations or high RLs combined (possibly combined with a washing step after the loading step), while the number of empty pores could be reduced by either dispensing droplets with $RL_1 > 1.0$ on the chip or repeating the loading and washing sequence with droplets at low concentration and/or with an $RL_1 < 1.0$.

To investigate this in more detail, the TRL has been varied by changing the number of subsequent droplet additions N at two different concentrations ($c = 0.0025$ and 0.005 mg mL^{-1}). Two distinct sets of experiments were performed: one using multiple droplets with a $RL_1 = 0.6$ ($N = 2, 3$), the other using single droplets of $RL_1 = 1.2$. Notice that a single loading step of $RL_1 = 0.6$ is pointless as the TRL <1.

Although showing large standard deviations, the results in Fig. 3 show that the quality of the assembly is not necessarily improved by supplying particles in subsequent steps with $RL_1 = 0.6$ ($c = 0.005$ mg mL^{-1}), but may even be deteriorated by these multiple sequences. This holds in the horizontal operating mode both without and with washing step. Whereas the deteriorating quality is obvious without

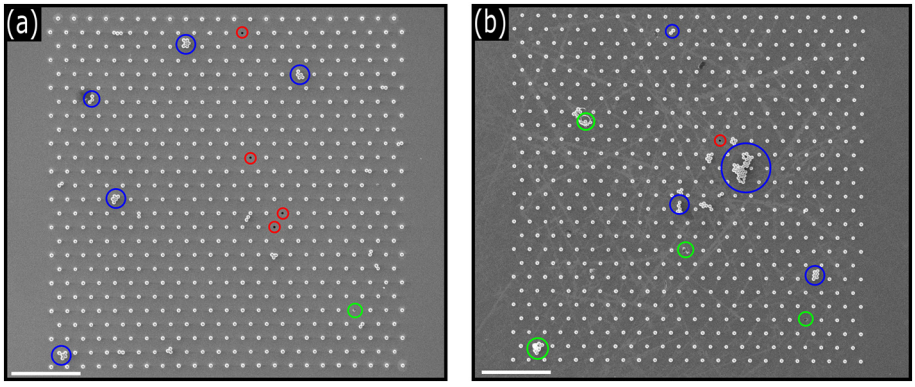

Fig. 2. SEM images of the assembled 10 μm silica particles on the orifices of membrane pores on the CF_x-coated chips placed in **(a)** the horizontal or **(b)** the vertical position. The blue circles indicate particle clusters, the red circles indicate empty pores, and the green circles indicate dust contamination. Conditions: silica particles dispersed in water with concentration $c = 0.005$ mg mL^{-1}, $RL_1 \approx 1.0$, membrane area 1.0×1.0 mm^2 and pitch $= 35$ μm. Scale bar $= 200$ μm.

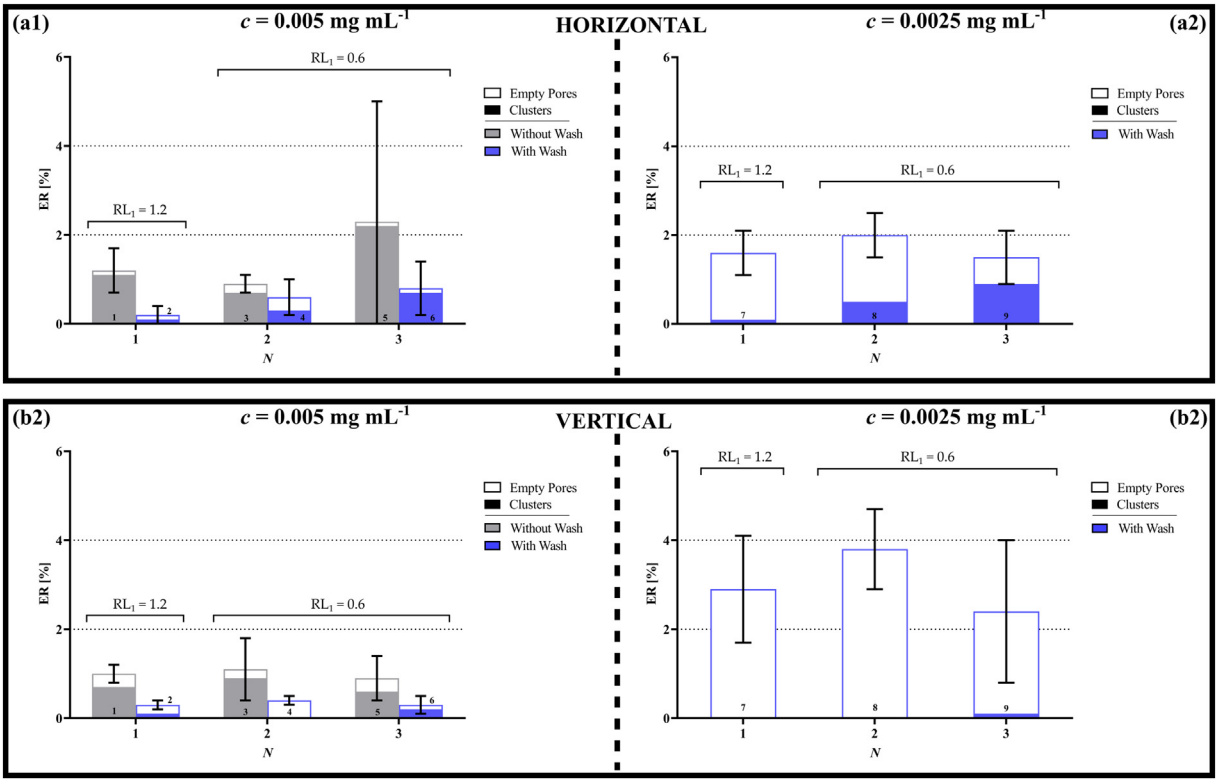

Fig. 3. Bar chart of the error ratio ER observed when depositing droplets comprising 10 μm silica particles with concentration $c = 0.0025$ mg mL^{-1} **(a2&b2)**, and 0.005 mg mL^{-1} **(a1&b1)** on CF_x-coated membranes with pitch $d = 35$ μm placed in either **(a)** horizontal or **(b)** vertical position as a function of the total number of cycles N. The RL_1 has been varied with the addition of washing steps (1 mL of water) after some cycles. The error bars represent the standard deviation for $n = 3$. Each bar contains the fraction of particle clusters (filled part of the bar) and empty pores (empty part of the bar).

washing step, it is less expected when a washing step is added. On the other hand, in the vertical operating mode when $c = 0.0025$ mg mL^{-1}, the number of empty pores is significantly reduced in the TRL > 1.0 case (cf. bars #7–9 in Fig. 3d) with respect to the RL ≅ 1.0 case (cf. bar #2 in Fig. S2). Hence, the quality of the assembly in the former case is considerably improved (ER = 2 − 4% vs. ER = 8%).

While the use of droplets with $RL_1 < 1.0$ inevitably leads to a high number of empty pores, Fig. 3a shows that, by adding multiple loading steps, the number of empty pores is significantly decreased with each step cf. bars #5, 6 and 9 in Fig. 3a) in the horizontal mode, while in the vertical mode significantly more pores remain unoccupied (cf. bars #5, 6 and 9 in Fig. 3b). The latter can be explained by the gravitational flow of the droplets, which inevitably transports the particles away from the membrane pores, bringing them too far away for the suction pores to become sufficiently attracted. Therefore, in the most diluted case, even a TRL = 1.8 ($N = 3$) did not resolve the problem of the large number of vacant pores in the vertical mode (cf. bar #9 in Fig. 3b2). This result suggests that, when only a few pores are left open, the available suction force becomes too weak to capture the particles that are being transported along the membrane by the induced flow. However, at higher concentrations the volume of the droplets are smaller, such that fewer particles can escape the applied suction force in the vertical mode, reducing the number of empty pores (compare bars #7–9 in Fig. 3b2 vs. bars #2, 4, 6 in Fig. 3b2).

On the other hand, the results also show that the fraction of clusters in the vertical mode remains relatively low compared to the horizontal mode. The reason for this is the fact that all particles are eventually attracted towards the membrane in the horizontal mode. As a consequence of the random distribution of the particles in the dispersion, this inevitably leads to the formation of clusters. In addition, there is no flow that may remove the formed clusters as is the case in the vertical mode. To take advantage of this observation, a washing step was added after each loading step to remove the formed particle clusters regardless of the operating mode. The ER-values in Fig. 3 indeed confirm that the addition of a washing step after each loading step substantially decreased the fraction of particle clusters on the membranes and the difference between the ER obtained with the $RL_1 = 0.6$ case and the $RL_1 = 1.2$ case becomes insignificant.

A caveat should be added here: subsequent loading steps increase the chance of dust particles blocking the pores, thus hindering the ordered array assembly of particles on the membrane. Therefore, single droplets with $RL_1 > 1$ seem to be more appropriate to obtain high quality assemblies than multiple additions of $RL_1 < 1$-droplets. The results in Fig. 3 support our hypothesis that an effective high RL around the membrane, depending on both concentration and chosen RL, decreases the number of empty pores, but promotes the formation of particle clusters significantly. Therefore, the addition of a flow is imperative to remove these formed clusters.

3.2. Effect of hydrophobic/hydrophilic nature of the surface

In addition to utilizing hydrophobic CF_X-coated silicon chips, experiments were also performed on non-coated silicon chips to test if the hydrophilicity of the surface affects the quality of the particle assembly. Fig. 4 displays the ER-data obtained after a single loading and washing sequence on the two different chip surfaces. The results show that the average ER's on the CF_X-coated chips are lower and more reproducible compared to what is obtained with the hydrophilic non-coated silicon chips.

In the horizontal mode, it seems that particles may have a higher tendency to form clusters on the silicon membranes compared to their CF_X-coated counterparts. This observation can be explained from studies published on the coffee-ring effect (CRE). In the CRE, particles dispersed in sessile droplets are driven by the capillary flow towards the

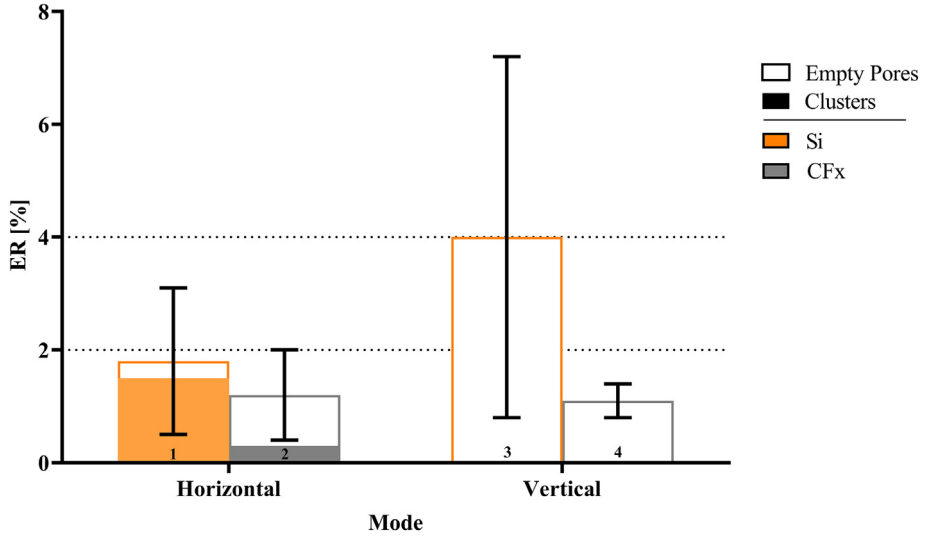

Fig. 4. Bar chart of the error ratio ER observed when depositing single water droplets comprising 10 μm silica particles with concentration $c = 0.005$ mg mL^{-1} and total $RL_1 = 1.2$ deposited on CF_x-coated or non-coated silicon chips in either horizontal or vertical position. A washing step with 1 mL of water was added after each loading step. The error bars represent the standard deviation for $n = 3$. Each bar contains the fraction of particle clusters (filled part of the bar) and empty pores (empty part of the bar).

contact line of evaporating droplets [30–32]. At this contact line, the particles are deposited and form clusters. In our setup, this capillary flow is eclipsed by the applied vacuum force. However, when the droplet is near to its complete vanishing point, the CRE could become pronounced on the non-coated silicon chip while the effect will always be less on the CF_X-coated chips. For it is well-known that hydrophobic surfaces may suppress the CRE due to a lower contact angle hysteresis [32,33].

In the vertical mode, a large fraction of pores remains empty on the non-coated silicon chips. Owing to the hydrophilic nature of the silicon chip (contact angle = 35°), the droplet wets a larger area around the membrane than is the case for the CF_X-coated chip (contact angle = 107°) [25,29]. Hence, a larger number of particles is transported away from the membrane as the droplet spreads, thus explaining the large fraction of unoccupied pores.

Considering both the wetting properties as well as the suppression of the CRE, it can hence be concluded that higher quality of ordered particle array assemblies can be obtained with the CF_X-coated chips compared to the non-coated silicon chips.

3.3. Effect of the pore pitch

In many applications [1,2,9,10,14,34], scientists and engineers strive to assemble particles in configurations with smaller pitches. Experiments comprising of a single loading and washing steps have therefore been performed on membranes with a shorter particle-to-particle distance (=pitch d) ranging from 1.25 – 35 μm. For all pitch values, except $d = 1.25$ μm, the ER-values are consistent with previous observations, with a large fraction of empty pores mostly observed in the vertical mode, and larger fractions of clusters mainly in the horizontal mode (cf. Fig. S5 in the SI). Significantly higher ER-values are obtained for the smallest pitch $d = 1.25$ μm with respect to other cases (ER = 25 ± 6% both in the horizontal and vertical operating mode), with large clusters present on the array of particles even after a single washing step (cf. inset Fig. S5 in the SI). Thus, a single washing step was insufficient to remove all the formed particle clusters.

Subsequently, the effect of the pore pitch distance was investigated using the most optimal conditions evolving from the preceding sections. I.e., all experiments were performed with single water droplets comprising dispersed silica particles with $RL_1 = 1.2$ and $c = 0.025$ mg mL^{-1} on the CF_X-coated chips. This concentration allows the supply of lower volume droplets, which raises the effective RL near the pores. After the disappearance of the droplet, four consecutive washing steps were added to ensure that the majority of, if not all, the clusters were removed.

Fig. 5 displays the SEM images of the particle assemblies obtained for varying pitch distances in the (a) horizontal or (b) vertical operating mode. For the cases (1–3), where the pitch $d \geq 12.5$ μm, the obtained ER's were <0.34%, with a perfect ordered particle assembly attained on the membrane with pitch $d = 35$ μm placed in the horizontal mode.

Figs. 5a4 and 5b4 demonstrate that the application of four washing steps removed the majority of the large clusters forming excess layers on top of the bottom layer, thus significantly improving the quality of the assembled particle array in case of the minimal-pitch array (compare ER ≈1% in Figs. 5a4 & b4 vs. ER = 25% in Fig. S5). The large clusters stem from the fact that the high pore density inevitably leads to a situation where the probability of multiple particles hindering each other when approaching their destination pore is greatly increased. As illustrated with a blue circle on the inset of Fig. 5, this leads to a situation wherein particles get more easily trapped between adjacent pores. Due to their size ($D = 10$ μm > $d = 1.25$ μm), these trapped particles inevitably partly block the adjacent pores such that other approaching particles are unable to assemble on those pores. Therefore, these poorly positioned particles leave the underlying pores open, which results in a persistent local suction flow, consequently serving as a nucleation seed for the formation of massive clusters (cf. inset Fig. S4). The quality of the particle assembly could in this case ($d = 1.25$ μm) be further enhanced by sequentially adding more loading steps to fill the unoccupied pores, provided enough washing steps are added to remove the large clusters.

Regarding the smallest pitch $d = 1.25$ μm, it is noteworthy that another defect might occur during the assembly process. When a particle with diameter ≥12 μm would be captured, the neighbouring pores would be blocked from capturing other particles, i.e., the neighbouring pores would remain empty. We have used highly monodisperse particles such that this effect can be neglected. However, when employing a suspension of particles with a dispersity >8%, this should definitely be taken into account, as the probability for this effect increases.

3.4. Effect of dispersant and particle properties

While the preceding experiments were carried out with aqueous silica dispersions, particles are also often dispersed in solvents with a

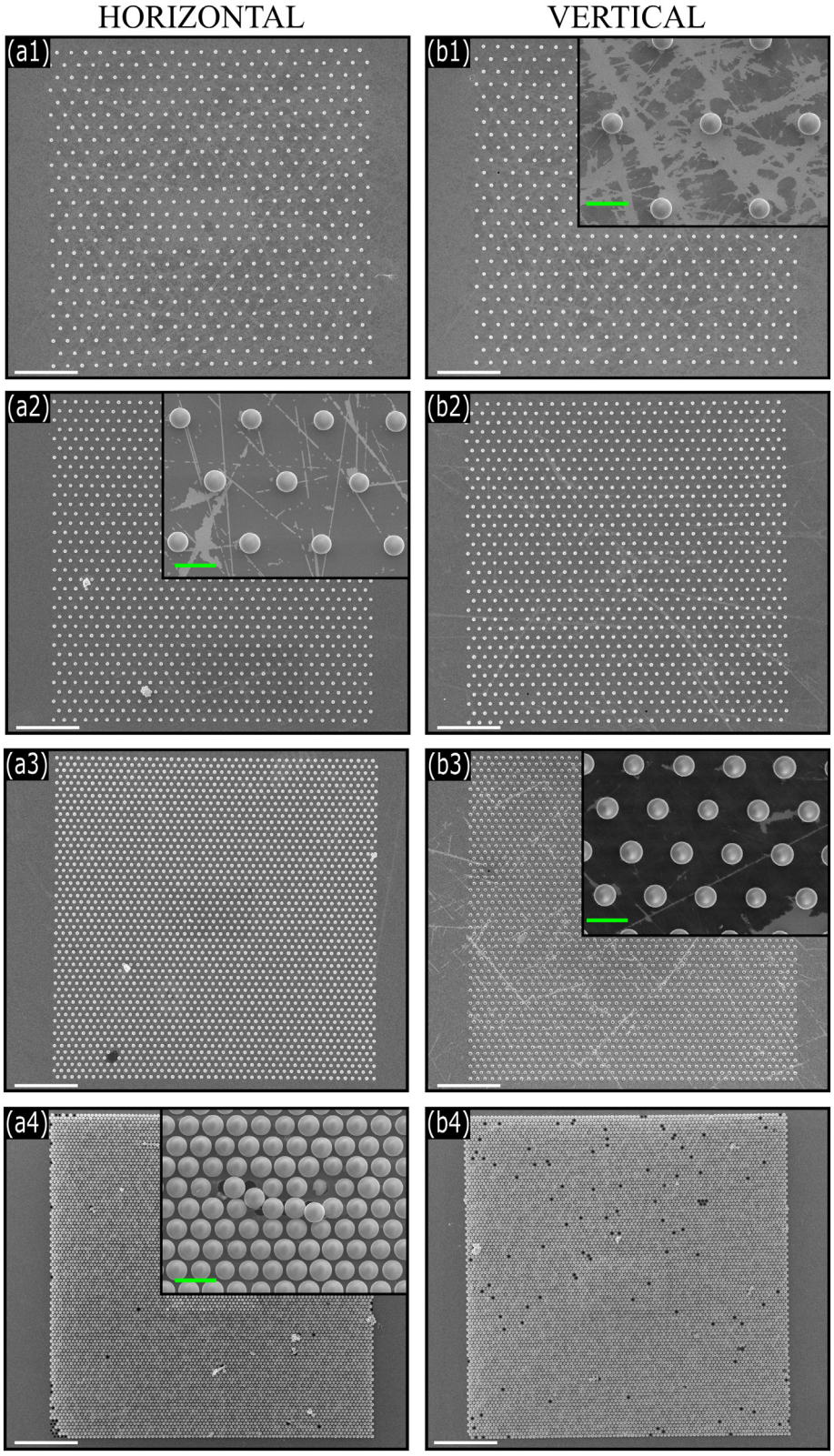

Fig. 5. SEM images of the monolayer assemblies attained on membranes with varying pitches: **(1)** 35 μm, **(2)** 23.75 μm, **(3)** 12.5 μm, and **(4)** 1.25 μm, placed in **(a)** the horizontal or **(b)** the vertical mode. Single water droplets with $RL_1 = 1.2$ $c = 0.025$ mg mL^{-1} were deposited on the CF_x-coated membranes. Four washing steps with 1 mL water droplets were performed after the loading step. The ER-values for the different cases are: **(a1)** = 0%, **(a2)** = 0.34%; **(b1)** = 0.10%, **(b2)** = 0.19%; **(c1)** = 0.10%, **(c2)** = 0.04%; **(d1)** = 0.66%, **(d2)** = 1.14%. The stripes visible in **(b1)** and **(a2)** are artifacts due to frequent cleaning of the chips in the ultrasonic bath. They were found to have no effect on the assembly process. White scalebar = 200 μm; green scalebar = 20 μm.

lower electrical permittivity than water to reduce the van der Waals forces or, if applicable, to reduce their hydrophobic-hydrophobic interactions. [35] To examine the universality of the proposed method, we therefore dispersed the hydrophilic silica or hydrophobic polystyrene (PS) particles in either ethanol or water. The obtained results are presented in Fig. 6. Note that, since the density of the PS particles is lower than that of the silica particles, the droplets containing PS particles are adapted to lower volumes (=56% of the volumes taken for the droplets containing silica particles) to keep RL constant.

The results for the silica particles show that the quality of the assembly obtained with ethanol after one cycle is inferior compared to that obtained with water, especially in the vertical mode. These observations can be explained by the fact that, owing to their lower contact angle, ethanol droplets disperse more laterally and hence also wet the surface next to the membrane. This lateral dispersion transports the particles away from the membrane, resulting in a lower effective RL, in turn leading to a substantially higher number of empty pores. This holds for the horizontal mode, but is most prevalent in the vertical mode. The results obtained with the PS particles dispersed in ethanol after one cycle in the horizontal mode (cf. bar #7 in Fig. 6a) support this hypothesis, as the effective loading near the membrane pores is significantly increased because of the lower volume ethanol droplet in the PS case. As a result,

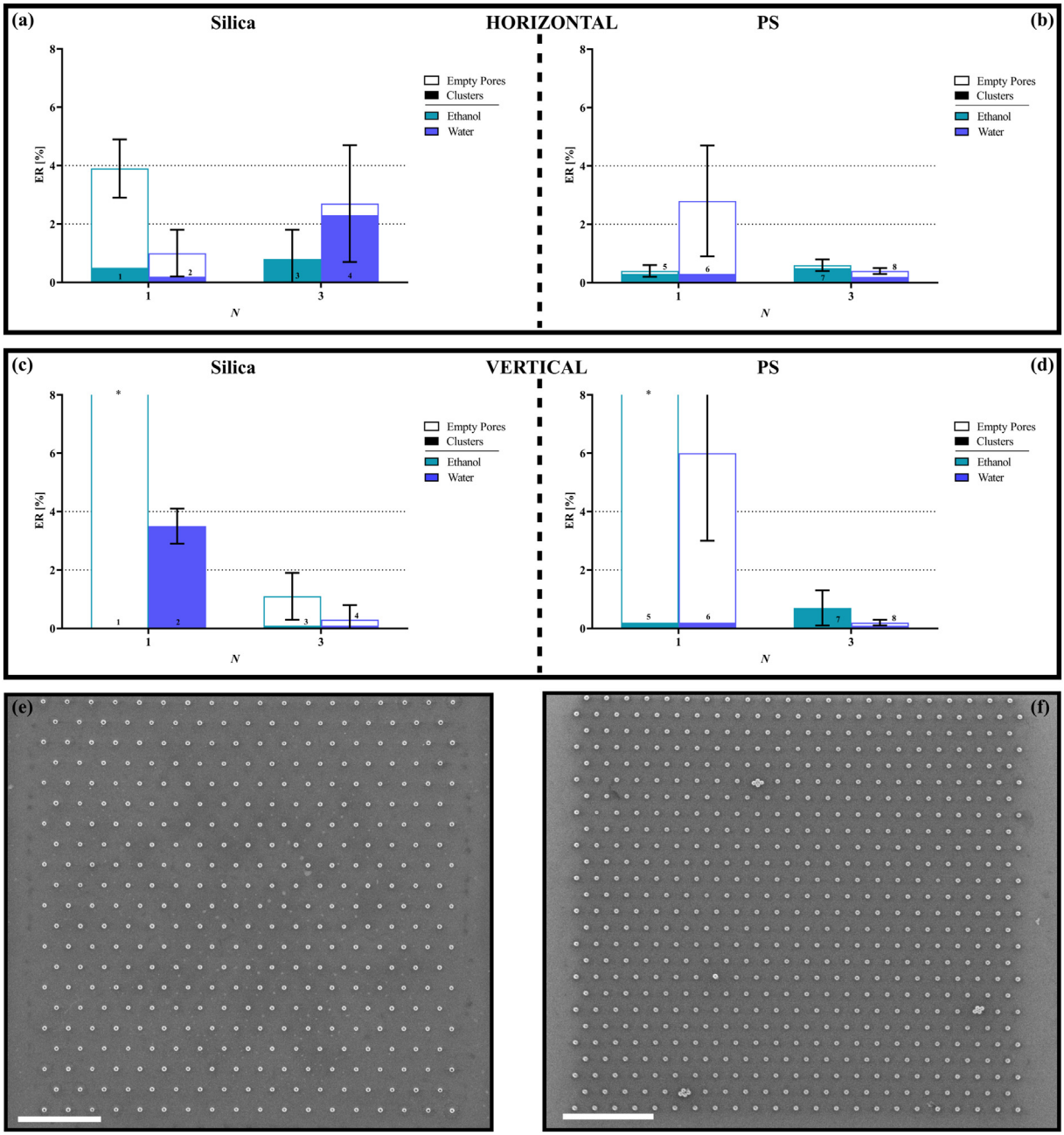

Fig. 6. Bar chart of the error ratio ER when dispensing single water or ethanol droplets comprising 10 μm **(a&c)** silica particles or **(b&d)** PS particles with concentration $c = 0.005$ mg mL^{-1} ($RL_1 = 1.4$) on the non-coated silicon chips with pitch = 40 μm (silica particles) or pitch = 35 μm (PS particles) placed in either **(a-b)** horizontal or **(c-d)** vertical position as a function of the total number of cycles *N*. Washing steps were added (either water or ethanol) after each loading step. In figure **(b)** the data for ethanol has been cut-off. The * represent a value of ER = 45%, i.e. off the scale of the graph. The error bars represent the standard deviation for $n = 3$. Each bar contains the fraction of particle clusters (filled part of the bar) and empty pores (empty part of the bar). A SEM image of one of the assemblies obtained with **(e)** silica particles in the vertical mode, and **(f)** PS particles in the horizontal mode, after three steps. Scale bar = 200 μm.

the number of vacant pores is substantially decreased. On the other hand, when the PS particles are dispersed in water, more pores remain empty compared to the silica particles after one sequence (compare bar #2 vs. #6 in Fig. 6a). Presumably, the hydrophobic-hydrophobic interactions in water drives the formation of PS particle clusters within the droplet/solution, resulting in a depletion of single particles available to occupy the empty pores.

Another effect originates from the fact that ethanol is more volatile than water. As the ethanol film evaporates much more rapidly, the time slot during which the vacuum force can attract the particles towards the membrane pores is significantly reduced. Because of the rapidly evaporating ethanol film the deposition of particles outside the membrane area may be promoted, which results in another depletion of particles.

To reduce the substantial number of empty pores observed in the discussed ethanol droplet cases, a refill sequence comprising multiple loading and washings steps was established for the two different dispersant and particle types. In the horizontal mode, the quality of the silica particle assembly with ethanol droplets is significantly improved after three cycles, whereas the quality attained with the water droplets deteriorated (Fig. 6a-b). The latter can be explained by the fact that, in this case, the majority of the pores is already occupied after a single step. As a consequence, the formation of clusters is promoted when subsequent steps are added. For the PS particles on the other hand, the quality of the assembly is improved after three steps (e.g., Fig. 6f), while the ER obtained with ethanol shows a slight, but insignificant, increase (Fig. 6b).

In the vertical mode (Fig. 6c-d), the quality of the assembly significantly improved with increasing N for both the silica as well as the PS particles. The results obtained for $N = 3$ for silica particles in water droplets in the vertical mode (e.g., Fig. 6e) show the importance of the induced flow as the fraction of clusters is substantially decreased (Fig. 6c). Thus, in this case (cf. bar #4 in Fig. 6c), the quality of the assembly is almost perfect, confirming the result shown in Fig. 3c (cf. bar #6) within the error margin.

From the results in Fig. 6a, it can be inferred that in the case of the silica particles a single loading step with water droplets (cf. bar #2) is sufficient to obtain the same assembly quality compared to the three steps with ethanol droplets (cf. bar #3). However, in the case of the PS particles, a more perfect assembly is obtained after a single cycle with ethanol than with water. Consequently, water droplets are preferred for the assembly of silica particles, whereas ethanol is the preferred dispersant for the assembly of the PS particles.

3.5. Transfer of the assembled array of silica particles

As the vacuum force can be switched off after the assembly process, the array of assembled microparticles is readily available for subsequent transfer on another substrate, provided that the substrate exerts a sufficiently strong net adhesion force on the assembled array. In a previous study [29], we have shown that silica particles can be transferred from a CF_X-coated surface onto a PDMS (20:1 *w*/w) slab. Using a similar approach, we attempted to transfer the assembled array of particles onto a PDMS sheet.

As can be observed from Fig. 7, particle transfer can indeed be realized by manually pressing the PDMS sheet on the assembled array, maintaining their initial position on the perforated device. Future research is required to investigate the most optimal conditions to transfer the particles on PDMS as well as other polymer surfaces. The transfer of the assembled array of particles can be advantageous for soft/flexible electronic devices [10,26].

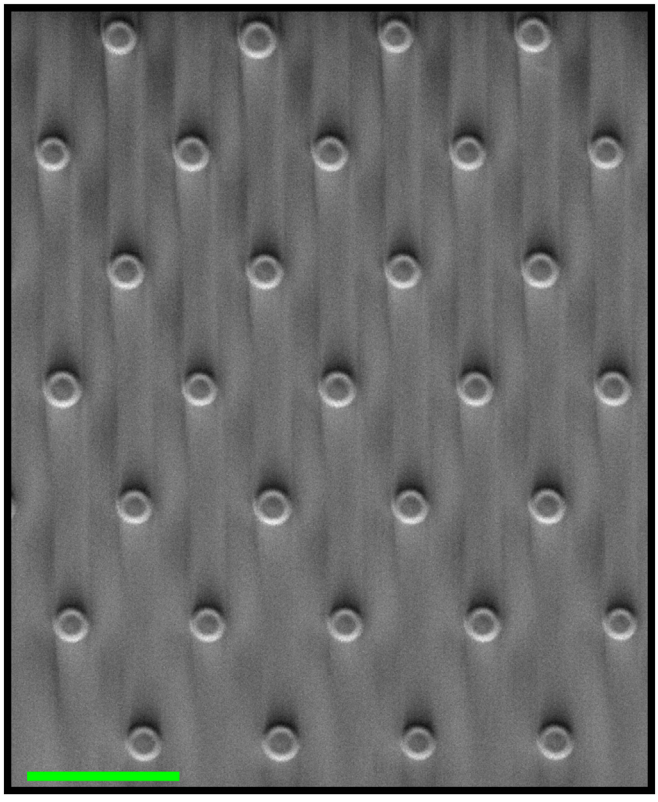

Fig. 7. SEM image of a transferred array of 10 μm silica particles from a CF_x coated membrane with a pitch of d = 45 μm onto a PDMS (20:1 *w*/w) sheet. The PDMS sheet has been pressed manually on the assembled array of silica particles. Scale bar = 50 μm.

4. Conclusion

In this study, a universal method is proposed to assemble an ordered array of microparticles on the surface of a micromachined grid of membrane pores. Droplets containing either silica particles ($9.98 \pm 0.31\ \mu$m) or PS particles ($9.98 \pm 0.11\ \mu$m) are dispensed on membranes connected to a vacuum pump. As the applied vacuum force sucks the dispersant through the membrane, the particles are captured on the array of pores. In general, the quality of the ordered array is impaired by three apparent defects: particle clusters, empty pores, or the interference of dust contamination. Occurrence of dust particles is random and will eventually be minimized in a dust-free working environment, therefore it is neglected in the interest of this study. We have studied the effect of various parameters on the quality of the obtained particle array with the proposed method.

The experiments were performed in a horizontal or vertical operating mode, each with its own advantages and disadvantages. In the horizontal mode, the number of vacant pores is minimized, but the formation of clusters is promoted, while in the vertical mode, the gravitation force-induced flow removes the particle clusters but transports particles away from the membranes, thus prompting a higher fraction of empty pores.

For the particles dispersed in water, we have varied the concentration c, the total relative loading TRL, and the wetting properties of the chips, amongst others. Altogether these studies highlighted that a high effective RL near the pores is required to decrease the number of empty pores with the addition of a crucial washing step to remove the particle clusters.

In addition, we have demonstrated that the proposed method is universal, as ordered array particle assemblies were attained with silica as well as PS particles dispersed in both ethanol or water, reporting promising ER's as low as $0.3 \pm 0.1\%$ for silica and $0.2 \pm 0.1\%$ for PS particles (pitch $d = 35\ \mu$m).

A drawback of the proposed method was pointed out when experiments were performed to assemble particles in a configuration with the smallest pitch $d = 1.25\ \mu$m. In this case, the quality of the particle

assembly can be significantly deteriorated, as particles can more easily compete for the same pore and some get trapped between adjacent pores, resulting in ER-values up to at least 25%. However, by using the optimal process parameters in conjunction with the addition of multiple washing steps, the overall quality of the formed particle array could be improved substantially leading to ER-values ≤ 1.14%.

Owing to the reversible nature of the applied vacuum force, the method potentially allows to manipulate, release, and subsequently transfer the assembled microparticle array. This makes the proposed method attractive for applications such as (soft-) electronic devices, cellular assays, sorting of (nonvolatile aerosol) particles, colloidal lithography, and fabrication of microsieves. In addition, the proposed method allows for the potential stamping of multiple assembled arrays onto another surface, which could be advantageous to manufacture microlens arrays or photonic films. Furthermore, the assembled arrays could be stacked to obtain three-dimensional functional materials.

In the present study, we solely studied the assembly of 10 μm particles using the proposed method. In principle, the method can be relatively easily extended to smaller sized particles after adjusting the pore diameter of the perforated device. However, it can be expected that, when going towards sub-micrometer or nanoparticles, the interparticle forces, e.g., the van der Waals forces, could dominate such that clusters of particles will already be formed within the dispersion, reducing the quality of the assembled array of particles. The assembly of nanoparticles hence remains to be studied.

Finally, it should be remarked that depending on the application, a trade-off exists between the diameter of the particle and optimal pore size. If the pore's orifice is too small, the particles and solvent will be insufficiently attracted to the pores, resulting in an impaired array of assembled particles. A separate series of experiments found that these 10 μm monodisperse particles also assembled on pores with a diameter down to 4 μm. Presumably, once the particles are trapped, the quality of the assembled array is not significantly affected. On the other hand, a larger pore diameter induces a sufficiently strong force, preventing undesired mobilization of the captured particles during subsequent manipulation or the crucial washing steps in the assembly process. In addition, for the successful transfer of particles to another surface, as demonstrated here, the pore diameter should not be too large. Moreover to prevent clogging, the pore's diameter should not exceed the diameter of the smallest particles. Considering all these constraints, we performed the experiments presented in this study with membranes carrying pores with a diameter of 7.5 μm.

Supplementary data to this article can be found online at https://doi.org/10.1016/j.powtec.2021.05.079.

Declaration of Competing Interest

The authors declare that they have no known competing financial interests or personal relationships that could have appeared to influence the work reported in this paper.

Acknowledgement

The authors gratefully acknowledge funding from the ERC Advanced Grant “Printpack” (No. 695067).

References

[1] N. Vogel, M. Retsch, C.-A. Fustin, A. del Campo, U. Jonas, Advances in colloidal assembly: the design of structure and hierarchy in two and three dimensions, Chem. Rev. 115 (2015) 6265–6311.
[2] Y. Wang, M. Zhang, Y. Lai, L. Chi, Advanced colloidal lithography: from patterning to applications, Nano Today 22 (2018) 36–61.
[3] J.F. Galisteo-López, M. Ibisate, R. Sapienza, L.S. Froufe-Pérez, Á. Blanco, C. López, Self-assembled photonic structures, Adv. Mater. 23 (2011) 30–69.
[4] A. Esmanski, G.A. Ozin, Silicon inverse-opal-based macroporous materials as negative electrodes for lithium ion batteries, Adv. Funct. Mater. 19 (2009) 1999–2010.
[5] S.M. Yang, H. Miguez, G.A. Ozin, Opal circuits of light—planarized microphotonic crystal chips, Adv. Funct. Mater. 12 (2002) 425–431.
[6] Y.-J. Lee, P.V. Braun, Tunable inverse opal hydrogel ph sensors, Adv. Mater. 15 (2003) 563–566.
[7] J.S. Choi, S. Bae, K.H. Kim, T.S. Seo, A large-area hemispherical perforated bead microarray for monitoring bead based aptamer and target protein interaction, Biomicrofluidics 8 (2014) 064119.
[8] B. Schurink, R. Tiggelaar, J. Gardeniers, R. Luttge, Fabrication and characterization of microsieve electrode array (μsea) enabling cell positioning on 3d electrodes, J. Micromech. Microeng. 27 (2016) 015017.
[9] K.R. Phillips, C.T. Zhang, T. Yang, T. Kay, C. Gao, S. Brandt, L. Liu, H. Yang, Y. Li, J. Aizenberg, et al., Fabrication of photonic microbricks via crack engineering of colloidal crystals, Adv. Funct. Mater. (2019) 1908242.
[10] H. Hwang, U. Jeong, Microparticle-based soft electronic devices: toward one-particle/one-pixel, Adv. Funct. Mater. (2019) 1901810.
[11] Y. Wang, Y. Yu, J. Guo, Z. Zhang, X. Zhang, Y. Zhao, Bio-inspired stretchable, adhesive, and conductive structural color film for visually flexible electronics, Adv. Funct. Mater. 30 (2020) 2000151.
[12] C. Hong, S. Yang, J.C. Ndukaife, Stand-off trapping and manipulation of sub-10 nm objects and biomolecules using opto-thermo-electrohydrodynamic tweezers, Nat. Nanotechnol. (2020) 1–6.
[13] V. Lotito, T. Zambelli, Pattern detection in colloidal assembly: a mosaic of analysis techniques, Adv. Colloid Interf. Sci. 102252 (2020).
[14] J. Zhang, Y. Qin, Y. Shen, C. Jiang, Y.-T. Tao, S. Chen, B.B. Xu, Z. Yu, Sessile microdroplet-based writing board for patterning of structural colored hydrogels, Adv. Mater. Interfaces 2001201 (2020).
[15] S.J. Strydom, D.P. Otto, N. Stieger, M.E. Aucamp, W. Liebenberg, M.M. de Villiers, Self-assembled macromolecular nanocoatings to stabilize and control drug release from nanoparticles, Powder Technol. 256 (2014) 470–476.
[16] U. Olgun, V. Sevnç, Evaporation induced self-assembly of zeolite a micropatterns due to the stick–slip dynamics of contact line, Powder Technol. 183 (2008) 207–212.
[17] H. Fang, M.O. Tadé, Q. Li, A numerical study on the role of geometry confinement and fluid flow in colloidal self-assembly, Powder Technol. 214 (2011) 283–291.
[18] S. Ni, L. Isa, H. Wolf, Capillary assembly as a tool for the heterogeneous integration of micro-and nanoscale objects, Soft Matter 14 (2018) 2978–2995.
[19] K.D. Barbee, A.P. Hsiao, E.E. Roller, X. Huang, Multiplexed protein detection using antibody-conjugated microbead arrays in a microfabricated electrophoretic device, Lab Chip 10 (2010) 3084–3093.
[20] X. Chen, T.F. Leary, C. Maldarelli, Transport of biomolecules to binding partners displayed on the surface of microbeads arrayed in traps in a microfluidic cell, Biomicrofluidics 11 (2017) 014101.
[21] N.V. Dziomkina, M.A. Hempenius, G.J. Vancso, Symmetry control of polymer colloidal monolayers and crystals by electrophoretic deposition on patterned surfaces, Adv. Mater. 17 (2005) 237–240.
[22] B. Bharti, F. Kogler, C.K. Hall, S.H. Klapp, O.D. Velev, Multidirectional colloidal assembly in concurrent electric and magnetic fields, Soft Matter 12 (2016) 7747–7758.
[23] A. Jonáš, P. Zemanek, Light at work: the use of optical forces for particle manipulation, sorting, and analysis, Electrophoresis 29 (2008) 4813–4851.
[24] S.M. Weekes, F.Y. Ogrin, W.A. Murray, P.S. Keatley, Macroscopic arrays of magnetic nanostructures from self-assembled nanosphere templates, Langmuir 23 (2007) 1057–1060.
[25] I.S.M. Jimidar, K. Sotthewes, H. Gardeniers, G. Desmet, A detailed study of the interaction between levitated microspheres and the target electrode in a strong electric field, Powder Technol. (2021) https://doi.org/10.1016/j.powtec.2021.01.036.
[26] K. Koh, H. Hwang, C. Park, J.Y. Lee, T.Y. Jeon, S.-H. Kim, J.K. Kim, U. Jeong, Large-area accurate position registry of microparticles on flexible, stretchable substrates using elastomer templates, ACS Appl. Mater. Interfaces 8 (2016) 28149–28158.
[27] C. Py, M. Martina, G.A. Diaz-Quijada, C.C. Luk, D. Martinez, M.W. Denhoff, A. Charrier, T. Comas, R. Monette, A. Krantis, et al., From understanding cellular function to novel drug discovery: the role of planar patch-clamp array chip technology, Front. Pharmacol. 2 (2011) 51.
[28] H.V. Jansen, J.G. Gardeniers, J. Elders, H. Tilmans, M. Elwenspoek, Applications of fluorocarbon polymers in micromechanics and micromachining, Sens. Actuators, A 41 (1994) 136–140.
[29] I. Jimidar, K. Sotthewes, H.J. Gardeniers, G. Desmet, Spatial segregation of microspheres by rubbing-induced triboelectrification on patterned surfaces, Langmuir 36 (2020) 6793–6800.
[30] R.D. Deegan, O. Bakajin, T.F. Dupont, G. Huber, S.R. Nagel, T.A. Witten, Capillary flow as the cause of ring stains from dried liquid drops, Nature 389 (1997) 827–829.
[31] A.G. Marin, H. Gelderblom, D. Lohse, J.H. Snoeijer, Order-to-disorder transition in ring-shaped colloidal stains, Phys. Rev. Lett. 107 (2011) 085502.
[32] D. Mampallil, H.B. Eral, A review on suppression and utilization of the coffee-ring effect, Adv. Colloid Interf. Sci. 252 (2018) 38–54.
[33] L. Cui, J. Zhang, X. Zhang, Y. Li, Z. Wang, H. Gao, T. Wang, S. Zhu, H. Yu, B. Yang, Avoiding coffee ring structure based on hydrophobic silicon pillar arrays during single-drop evaporation, Soft Matter 8 (2012) 10448–10456.
[34] R. Xu, T. Zhou, R. Cheung, Fabrication of sic concave microlens array mold based on microspheres self-assembly, Microelectron. Eng. 236 (2021) 111481.
[35] H.-J. Butt, B. Cappella, M. Kappl, Force measurements with the atomic force microscope: technique, interpretation and applications, Surf. Sci. Rep. 59 (2005) 1–152.